Supporting Information

Colloidal Quasi-One-Dimensional Dual Semiconductor Core/Shell Nanorod Couple Heterostructures with Blue Fluorescence

Dechao Chen, Aixiang Wang, Hongbo Li, Laura Abad Galán, Cong Su, Zongyou Yin, Massimiliano Massi, Alexandra Suvorova, Martin Saunders, Ju Li, Amit Sitt,* Guohua Jia*

Experimental Section

Chemicals: $Zn(NO_3)_2 \cdot 6H_2O$ (99%), zinc diethyldithiocarbamate (97%), selenium powder (99.999%), CdO (99%), sulfur (99%), bis(trimethylsilyl)sulfide (98%), dodecanethiol (98%), oleylamine (approximate C_{18} content 80−90%), oleic acid (90%, technical grade), 1-octadecene (90%, technical grade), trioctylphosphine (TOP, 97%), trioctylphosphine oxide (TOPO, 90%), toluene (99.8%, anhydrous), chloroform (99%, anhydrous), and methanol (99.8% anhydrous) were purchased from Sigma-Aldrich. Octadecylphosphonic acid (ODPA) and hexylphosphonic acid (HPA) were purchased from PCI Synthesis. All chemicals were used as received without further purification.

Preparation of Zinc Precursor Stock Solution: A 0.067 M zinc stock solution was prepared by dissolved $Zn(NO_3)_2 \cdot 6H_2O$ (0.2 mmol) in oleylamine (10 mL) in a three-neck flask. The mixture was degassed and refilled with N_2 three times at room temperature and then heated to 110 °C and kept at this temperature under vacuum for 30 minutes. Then the mixture was further heated up to 160 °C and kept at this temperature for 30 minutes.

Synthesis of thin ZnSe nanorods: Thin ZnSe nanorods synthesis was conducted according to a previously reported approach with some modifications.[26] In a typical synthesis, 0.2 mmol (59.5 mg) $Zn(NO_3)_2 \cdot 6H_2O$ and 10 mL oleylamine were mixed in a three-neck flask. The mixture was degassed and refilled with N_2 three times at room temperature and then heated to 110 °C and kept at this temperature for 0.5 hour. At 160 °C, 2 mL 0.1 M Se oleylamine solution was injected into the flask. After the injection, the temperature was set at 120 °C and the mixture was degassed for 10 minutes. After the flask was refilled with N_2, the temperature was raised up to 230 °C in 6 minutes. After 20 minutes at 230 °C, the reaction was quenched by removing the heating mantle.

Purification of thin ZnSe nanorods: Purification of nanoparticles was conducted by dissolving 2 mL of the crude solution into 2 mL chloroform solution. Then methanol was continuously added into the solution until a turbid solution was obtained. The precipitation was separated from the solution by the aid of centrifugation and this procedure may repeat two or three times.

Synthesis of hetero- ZnS-ZnSe/ZnS core/shell Nanorod Couples: 30 mg purified thin ZnSe nanorods were dissolved in 15 mL oleylamine in a three-neck flask and then 4 mL 0.067 M zinc precursor stock solution was added into the flask. The mixture was degassed and refilled with N_2 three times at room temperature and then heated to 110 °C and kept at this temperature for 30 minutes under vacuum. Then the mixture was heated to 260 °C in 7 minutes. At 260 °C, 1 mL (4.17 mmol) of 1-dodecanethiol was injected into the flask. After the injection, the temperature was raised to 280 °C in four minutes. After 30 minutes at 280 °C, the reaction was quenched by removing the heating mantle. Aliquots have been taken from time to time to monitor the growth of nanoparticles. Other sulfur source, such as (4.0 mmol) bis(trimethylsilyl)sulfide, has been used to substitute 1-dodecanethiol for synthesis of branched nanorod couples. The synthetic conditions for the synthesis of hetero- ZnS-ZnSe/ZnS core/shell nanorod couples using bis(trimethylsilyl)sulfide as the sulfur source are exactly same as above except 1-dodecanethiol has been replaced by bis(trimethylsilyl)sulfide.

Synthesis of homo- ZnSe Nanorod Couples: The synthesis of homo- ZnSe nanorod couples was conducted according to a previously reported approach with some modifications.[26] In a typical synthesis, 30 mg purified thin ZnSe nanorods was dissolved into 15 mL oleylamine solution into a three-neck flask. 1 mL 0.067 M zinc oleylamine and 1 mL 0.067 M selenium oleylamine stock solutions were added the flask at room temperature. Then the reaction solution was gradually heated up to 280 °C in 15 minutes and kept at this

temperature for 30 minutes. The reaction was quenched by removing the heating mantle. Aliquots have been taken from time to time to monitor the growth of nanoparticles.

Etching of ZnSe Nanorods: 30 mg purified thin ZnSe nanorods were synthesized by a reported approach[26,44] and were dissolved in 15 mL oleylamine in a three-neck flask and then 4 mL 0.067 M zinc precursor stock solution was added into the flask. The mixture was degassed and refilled with N_2 three times at room temperature for three times and then heated to 110 °C and kept at this temperature for 30 minutes under vacuum. Then the mixture was heated to 260 ºC in 7 minutes. At 260 °C, a certain amount of 1-dodecanethiol was injected into the flask. After the injection, the temperature was raised to 280 °C in four minutes. After 30 minutes at 280 °C, the reaction was quenched by removing the heating mantle. Aliquots have been taken from time to time to evolution of the nanoparticles.

Synthesis of ZnSe/ZnCdS Core/Shell Nanorod Couples: For the CdS shell growth, CdO (15 mg), trioctylphosphine oxide (2.0 g), octadecylphosphonic acid (75 mg) and hexylphosphonic acid (10 mg) were added to a three-neck flask (50 ml). The mixture was heated to 150 °C for 0.5 h under vacuum and then rise to 320 °C at N_2 to obtain a colourless solution. After that, the mixture was heated and stabilized at 365 °C and 3 ml TOP solution dissolved with 1×10^{-9} mol branched hetero- ZnS-ZnSe nanorod couples and 30mg sulfur was swiftly injected into the flask. After 30 seconds, the reaction was quenched by ice bathing. The crude reaction solution was diluted with toluene, methanol was added to precipitate the nanocrystals and remove excess surfactants.

Synthesis of Branched Hetero- PbS-PbSe Nanorod Couples: The cation exchange method was used to obtain branched hetero- PbS-PbSe nanorod couples from branched hetero- ZnS-ZnSe nanorod couples. A 0.05 M lead oleate stock solution was prepared by dissolving lead acetate (1 mmol) in a mixture of oleic acid (0.88 ml) and octadecene (19.12

4

ml) at 180 °C. The purified branched hetero- ZnS-ZnSe nanorod couples was dissolved in 1 mL anhydrous chloroform and then injected into 5 ml oleylamine in a 15 ml three-neck flask. After place in vacuum for 10 min, lead oleate stock (0.05 M) solution was injected into the flask and the temperature was raised to 100°C. After 5min at this temperature, the colorless solution transformed to dark brown, which indicates the Zn^{2+} ions have been substituted by Pb^{2+}. The solution was quenched by ice bathing and the obtained solution was washed by toluene and precipitated by methanol with the aid of centrifugation.

Synthesis of CdS rods: CdS nanorods were prepared using a literature method.[1] In a typical synthesis, CdO (60 mg), trioctylphosphine oxide (3.0 g), octadecylphosphonic acid (290 mg) and hexylphosphonic acid (45 mg) were added to a three-neck flask (50 ml). The mixture was heated to 150 °C for 0.5 h under vacuum and then rise to 320 °C at N_2 to obtain a colourless solution. After that, the mixture was heated and stabilized at 365 °C and 1.8 ml TOP solution dissolved with 4×10^{-8} mol CdS spherical dots and 60 mg sulfur was swiftly injected into the flask. After 9 minutes, the reaction was quenched by ice bathing. The crude reaction solution was diluted with toluene, methanol was added to precipitate the nanocrystals and remove excess surfactants with the aid of centrifugation.

Sample Characterization.

UV-vis Absorption Spectroscopy: UV-vis absorption spectroscopy was performed on a Perkin Elmer Lambda 35 UV/VIS Spectrometer using quartz cuvettes.

Photophysical measurements: Uncorrected steady-state emission spectra were recorded using an Edinburgh FLSP980-stm spectrometer equipped with a 450 W xenon arc lamp, double excitation and emission monochromators, a Peltier-cooled Hamamatsu R928P photomultiplier (185-850 nm). Emission spectra were corrected for source intensity (lamp and grating) and emission spectral response (detector and grating) by a calibration curve supplied with the

instrument. Overall quantum yields were measured with the use of an integrating sphere coated with BenFlect. Fluorescence emission lifetimes (τ) were determined with the time-correlated single photon counting technique (TCSPC) with the same Edinburgh FLSP920 spectrometer using pulsed picosecond LEDs (EPLED 280 or EPLED 320, FHWM <800 ps) as the excitation source, with repetition rates between 10 kHz and 1 MHz, and the above-mentioned R928P PMT as detector. To record the fluorescence spectra at 77 K, the samples were placed in quartz tubes (2 mm diameter) and inserted in a special quartz Dewar filled with liquid nitrogen. To measure the fluorescence spectra at different temperatures from 77 K to 287 K, the samples were placed in quartz cuvettes in a liquid nitrogen cryostat (Oxford Instrument). All the solvents used in the preparation of the solutions for the photophysical investigations were of spectrometric grade. Experimental uncertainties are estimated to be ±10% for lifetimes and ±20% for quantum yields.

XRD Measurement: XRD patterns were obtained using Cu Kα (λ=1.5406 Å) photons from an X'per PRO (PANalytical) X-ray diffractometer operated at 40 kV and 40 mA. Samples were deposited as a thin layer on a low-background scattering quartz substrate.

TEM *Measurement*: TEM grids were prepared by depositing one drop of a solution of purified nanoparticles onto a standard carbon coated grid. TEM was performed using a JEOL 2100 transmission electron microscope with a tungsten filament running at an accelerating voltage of 120 keV. HRTEM, HAADF-STEM, High-resolution *Z*-contrast STEM and STEM-energy-dispersive X-ray spectroscopy (EDX) were performed on an FEI Titan G2 80-200 high-resolution transmission electron microscope running at an accelerating voltage of 200 keV with a field emission gun as an electron source.
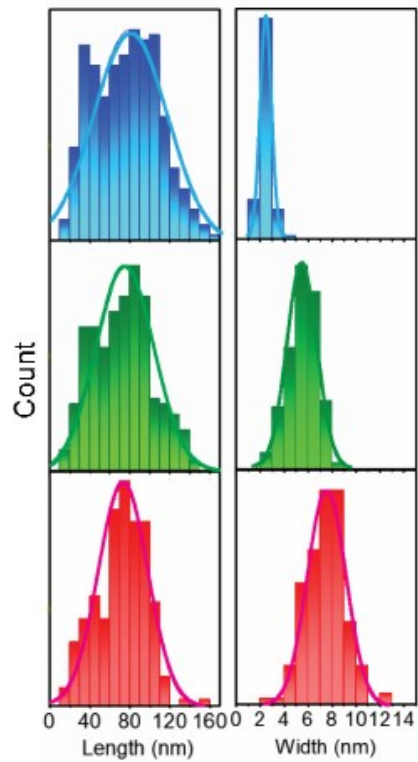
Figure S1. Sizing histograms of original ZnSe nanorods (top panel), hetero- ZnS-ZnSe/ZnS nanorod couples obtained after 30 seconds at 280 °C (middle panel), and branched hetero-ZnS-ZnSe/ZnS nanorod couples obtained after 30 minutes at 280 °C (bottom panel).
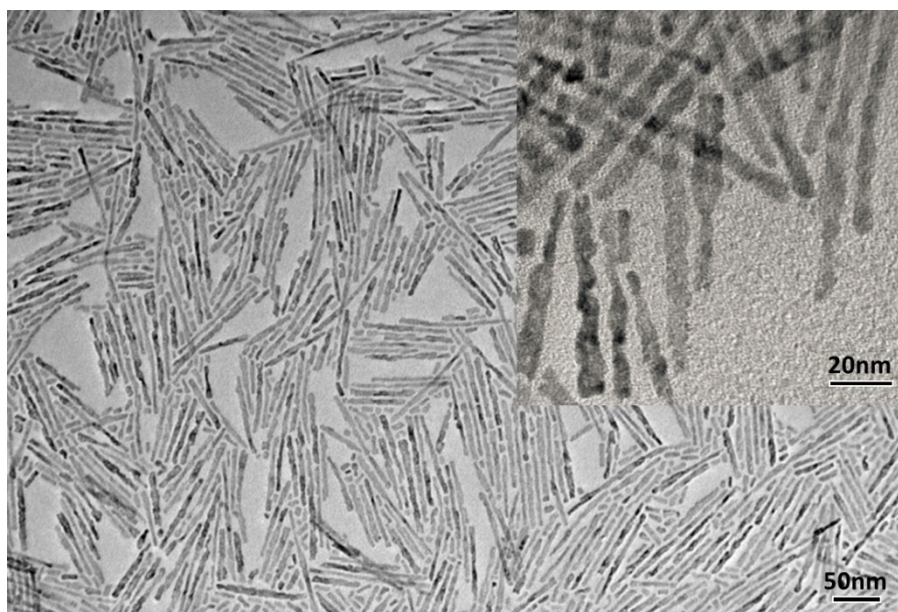
Figure S2. TEM image of hetero- ZnS-ZnSe/ZnS core/shell nanorod couples synthesized using bis(trimethylsilyl)sulfide as the sulfur source. Inset show a zoom-in of nanoparticles.
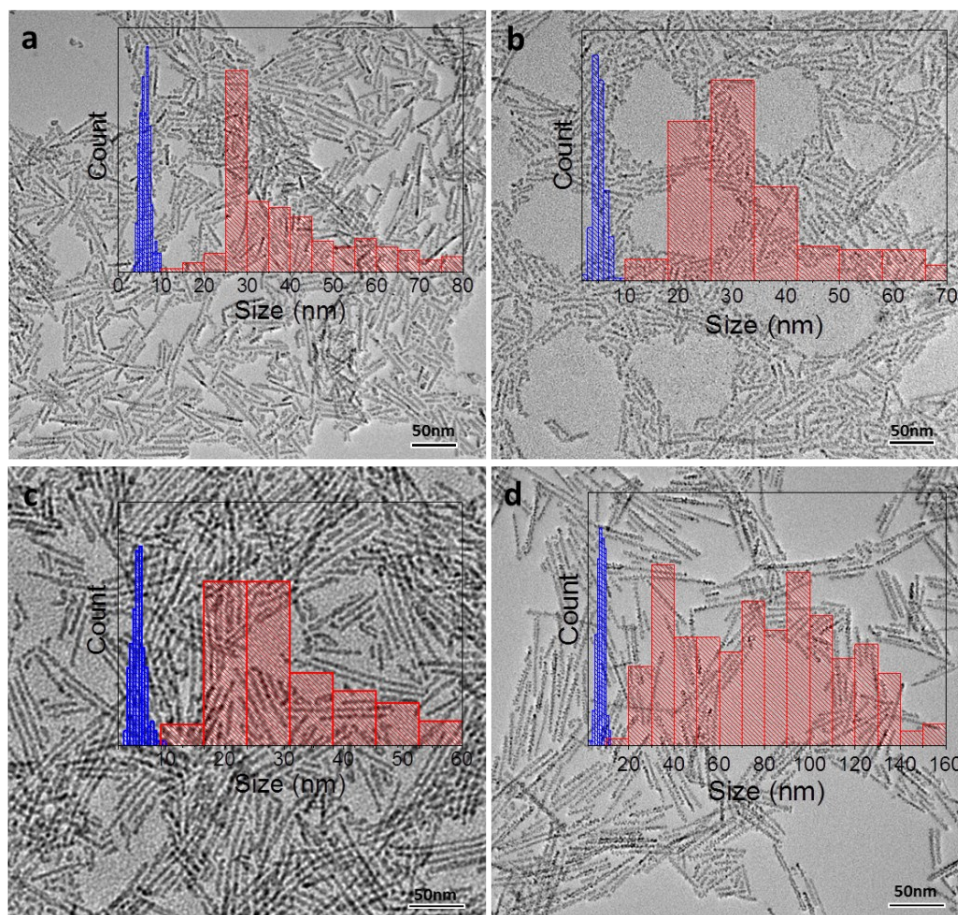
Figure S3. TEM images and sizing histograms of branched hetero- ZnS-ZnSe/ZnS nanorod couples with different dimensions. (a) Length (42.3±17.9 nm) × width (6.3±1.2 nm). (b) Length (37.7±20.5 nm) × width (5.3±1.1 nm). (c) Length (45.1±23.4 nm) × width (5.4±1.1 nm). (d) Length (79.6±35.2 nm) × width (7.7±1.6 nm).

9
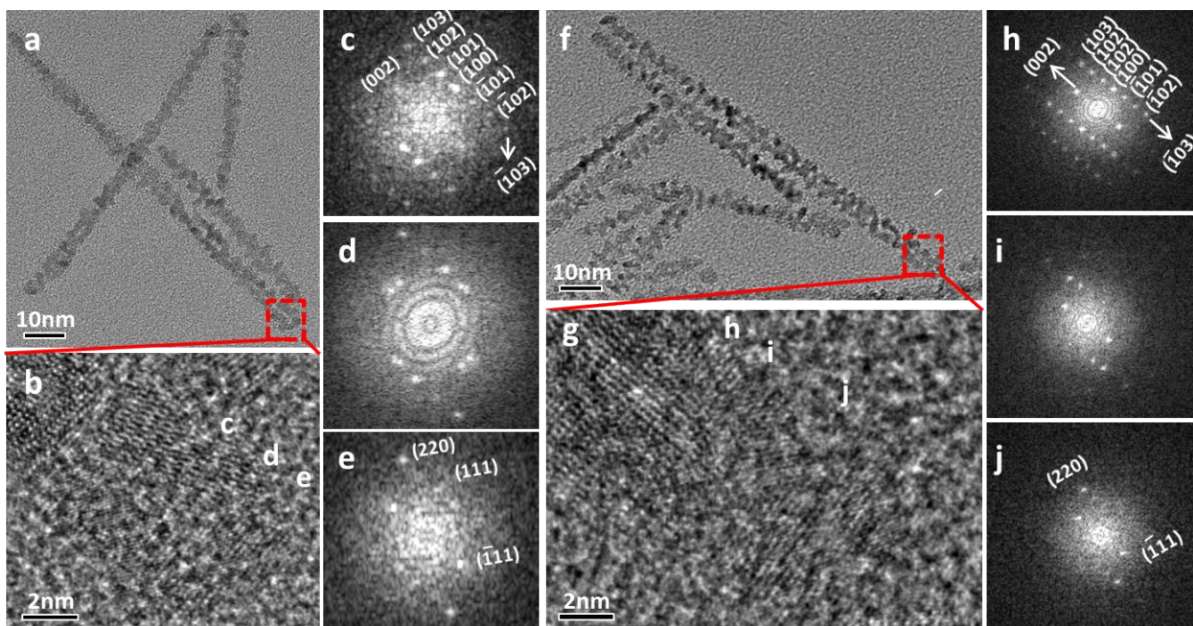
Figure S4. Electron microscopy imaging characterizations of hetero- ZnS-ZnSe/ZnS core/shell nanorod couples. (a) TEM image. (b) HRTEM image of the short arm labelled by dashed rectangle in (a), showing a hetero- nanorod couple is formed by the growth of zincblende ZnS between the end facets of two parallelly aligned wurtzite ZnSe nanorods. (c-e) FFT of selected areas in (b) revealing the crystallographic relations. The diffraction patterns in (c) and (e) match wurtzite ZnSe and zincblende ZnS, respectively. (d) shows the concurrence of above two sets of diffraction patterns. (f) TEM image. (g) HRTEM image of the short arm labelled by dashed rectangle in (f). (h-i) FFT of selected areas in (g) revealing the crystallographic relations. The diffraction patterns in (h) and (j) match wurtzite ZnSe and zincblende ZnS, respectively.

Table S1. Comparison of lattice mismatches of the nanostructures.

Initial material	(0002) wurtzite ZnSe	(0002) wurtzite ZnSe	(0002) wurtzite ZnSe
Second material	(111) zincblende ZnS	(0002) wurtzite ZnS	(0002) wurtzite CdS
Mismatch (%)	3.9[3]	4.5[4]	3.4[5,6]

The mismatches were calculated by the equation below:
Lattice mismatch = (lattice parameter of initial material – lattice parameter of a second material)/ lattice parameter of initial material.

The lattice plane spacings for (0002) of wurtzite ZnSe, (111) of zincblende ZnS, (0002) of wurtzite ZnS and (0002) of wurtzite CdS are 0.32500 nm, 0.3123 nm, 0.31292 nm and 0.33599 nm, respectively.
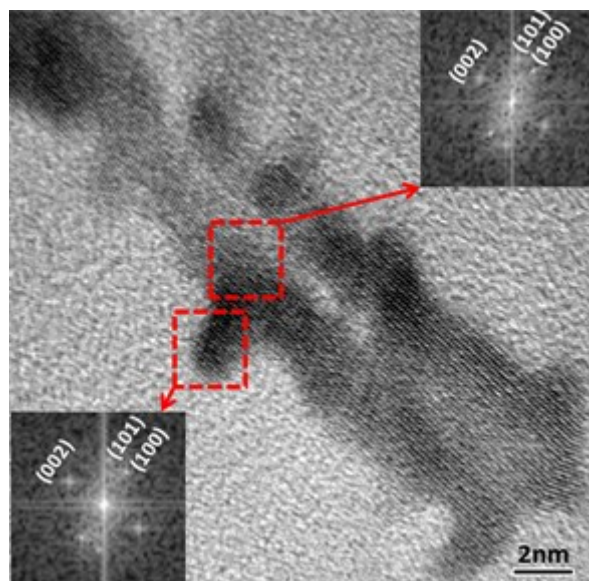
Figure S5. TEM images of "dual" nanorods showing the gap between two rod components. Insets show the FFT analyses of the selected areas.
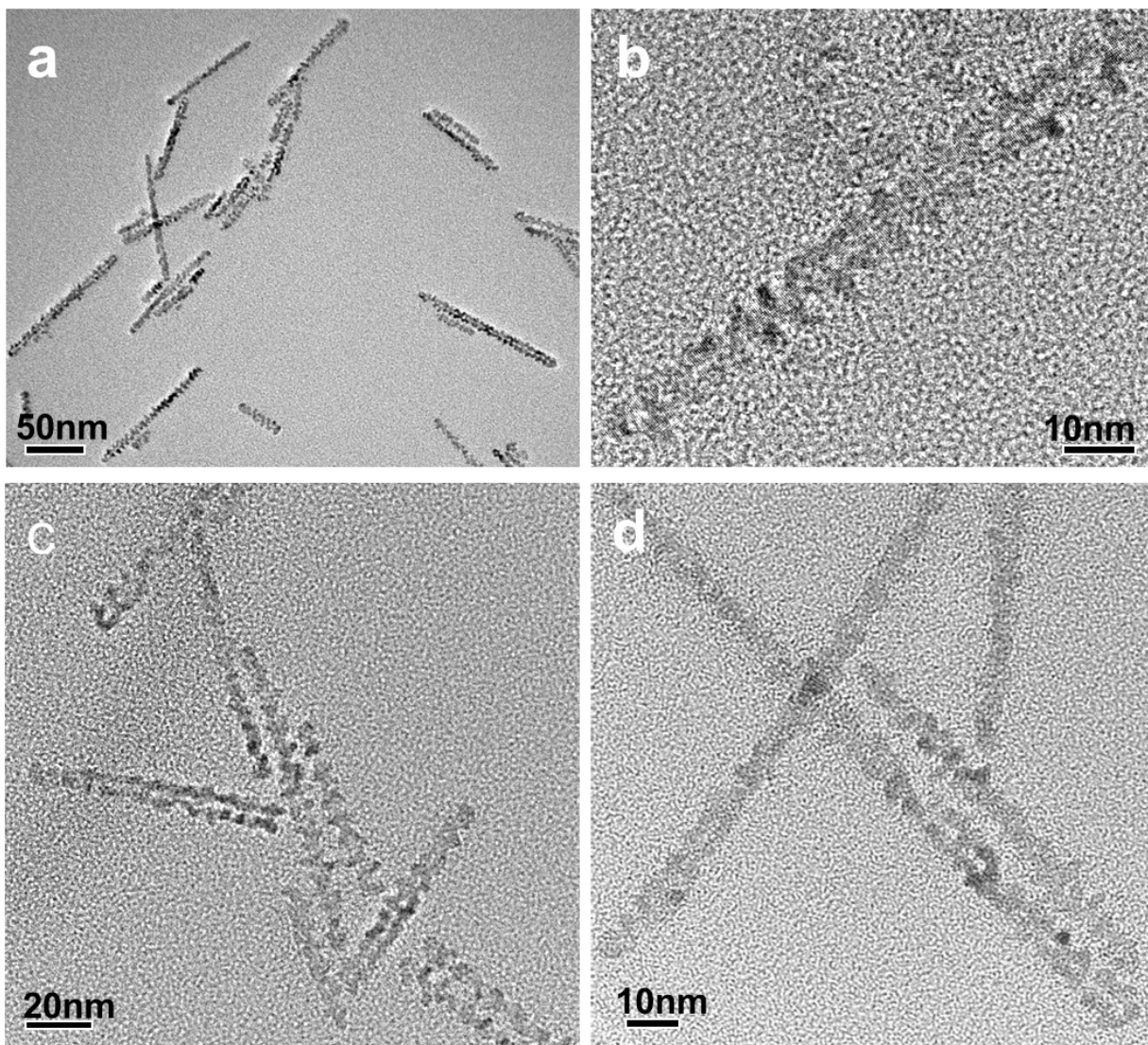
Figure S6. TEM images of hetero- ZnS-ZnSe/ZnS nanorod couples showing the gap between two rod components.
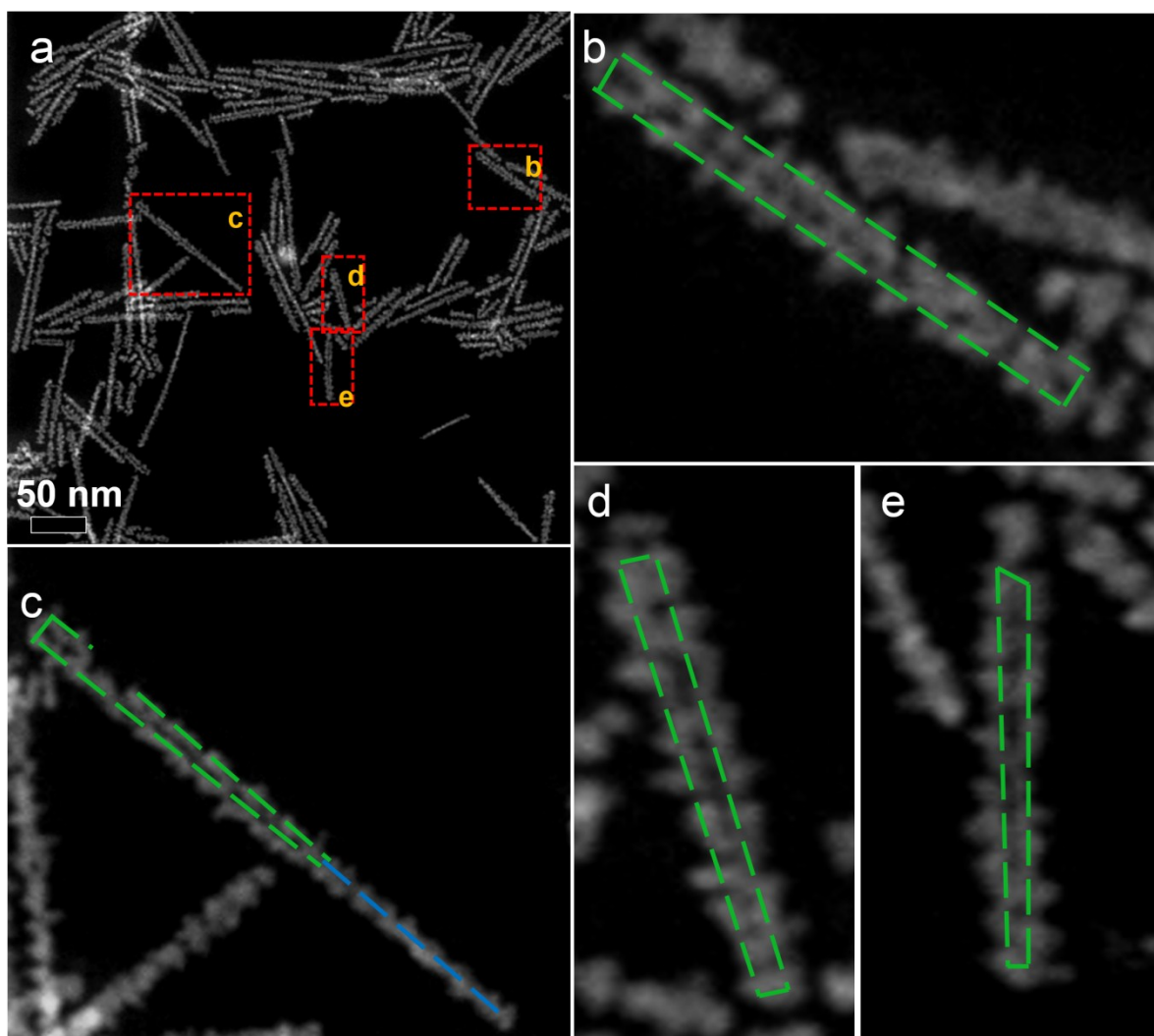
Figure S7. HAADF-STEM images showing the gap between two rod components of hetero- ZnS-ZnSe/ZnS nanorod couples. (a) Branched hetero- nanorod couples. (b-e) Enlarged images of individual nanoparticle as marked by red rectangles in (a). The green lines outline the long rod components, and blue line indicates single rod features of a branched nanorod couple which was formed due to partial coalesce of side facet of the "dual rods" occurred at elevated temperatures, e.g. 280 ^{o}C.
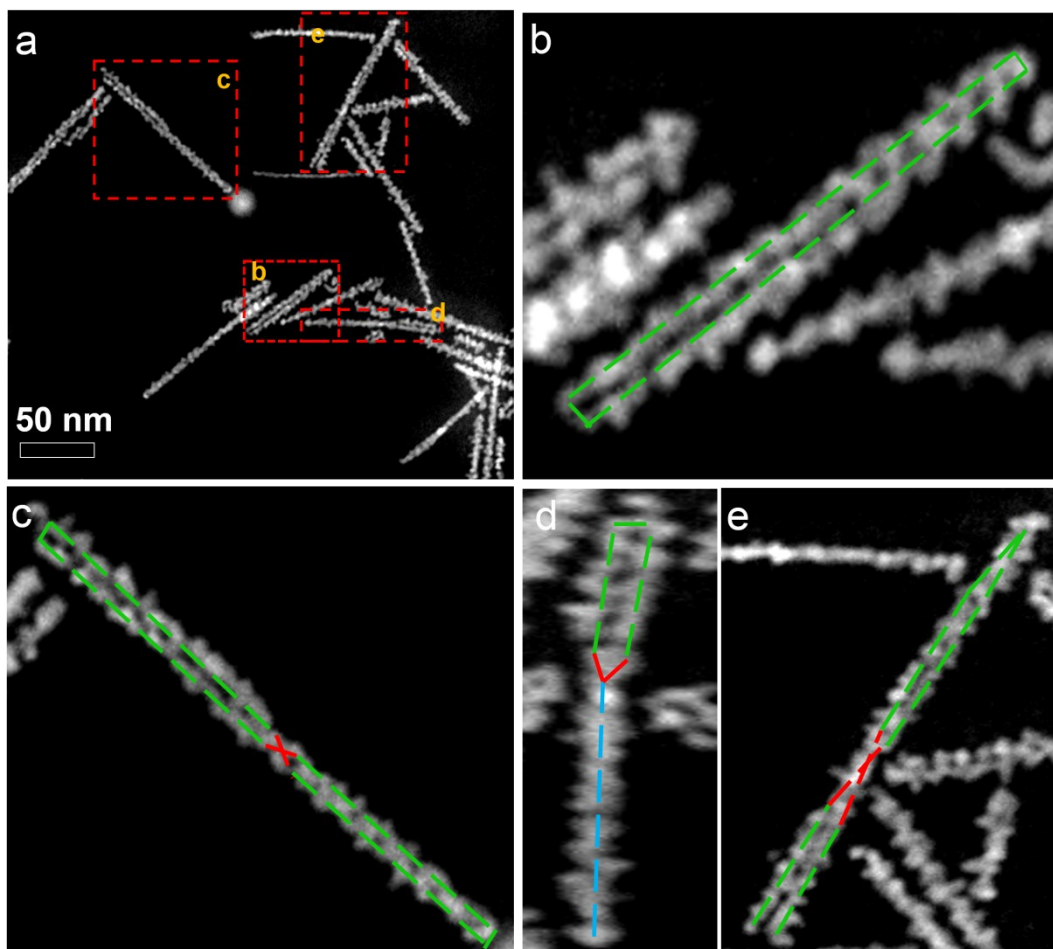
Figure S8. HAADF-STEM images of a) branched hetero- nanorod couples. b,c,d,e) Enlarged images of particles marked by red rectangles in a). The green lines outline the long rod components, and blue line indicates single rod features of a branched nanorod couple, and the red cross indicates the twist features of branched nanorod couples.

In general, the features of branched nanorod couples can be recognized with the guide of the green lines marked in the enlarged HAADF-STEM images. It is evident that the majority of branched nanorod couples remains the "dual rods" features. In Figure S7c and S8d, some parts of branched nanorods couples show single rod feature because of the partial coalesce of side facet of the "dual rods" occurred at elevated temperatures, e.g. 280 $^{\circ}$C. Other branched nanorods couples also show twisting, as marked by red cross, which is also observed in the previously reported ZnSe nanorod couples.[2]
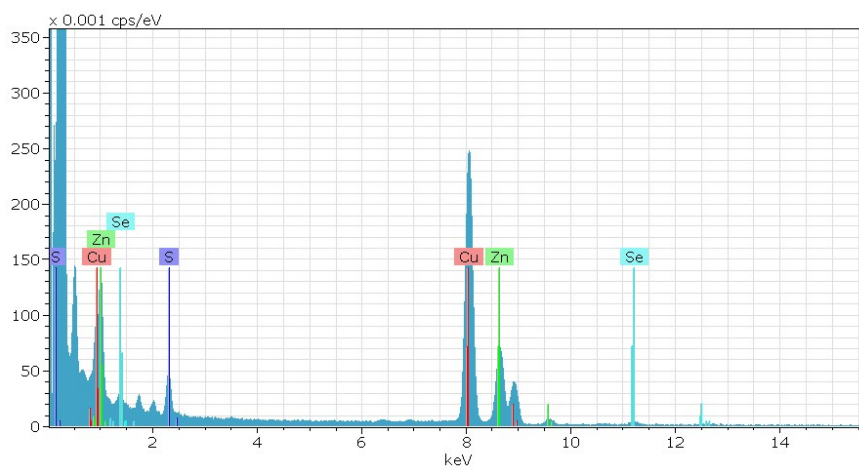
Figure S9. EDX spetrum of branched hetero- ZnS-ZnSe/ZnS core/shell nanorod couples confirming the presence of Zn, Se and S elements.
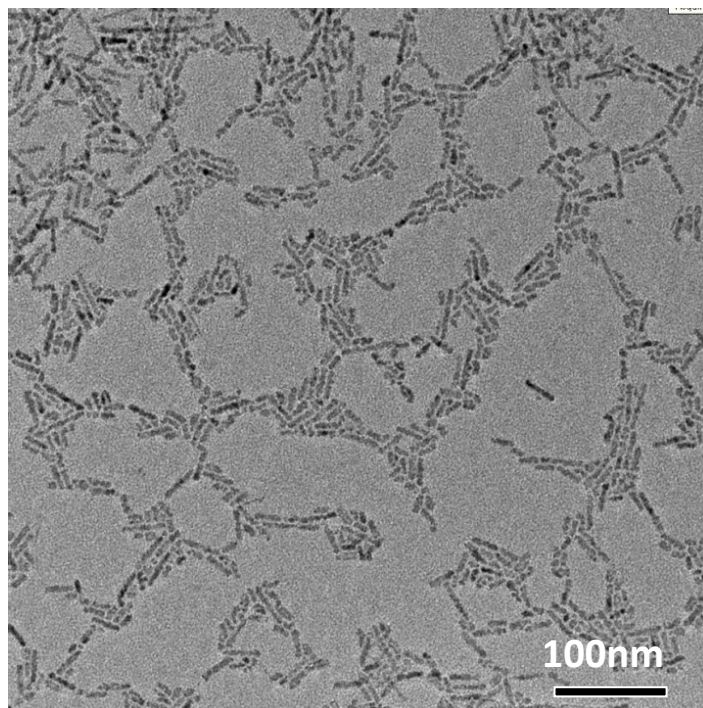
Figure S10. TEM images of etched ZnSe nanorod with rough surface facets obtained in oleylamine solution in the presence of 1-dodecanethiol after the reaction evolved for 30 minutes at 280 ^oC.

Electronic structure calculation

A finite well effective mass approximation (EMA) approach[7] was used to study the electronic structure of the hetero-ZnSe-ZnS/ZnSe core/shell nanorod couples, and in particular to compare them to that of homo- ZnSe nanorod couples. Due to the complex shape of the system, the solution was performed numerically using a finite element based model obtained with COMSOL Multiphysics package.

Within the EMA, we modeled the excited charge carrier confined to the particle as a particle in a box. Under this approximation, the Schrödinger equation for the electron (hole) envelope wave functions, φ_a, is defined as

$$\left(-\frac{h}{2m_a^*}\nabla^2 + V_a \right)\varphi_a = E_a\varphi_a, \qquad a = e/h \qquad (1)$$

where $\hbar$ is the reduced Planck constant, m_a^* is the reduced mass and V_a is the potential energy exerted on the charge carrier in the medium.

The total exciton energy can be calcualted by

$$E = E_{bg} + E_e + E_h \qquad (2)$$

where E_{bg} is the bulk's band gap. The potential energy of the charge carriers within the particle is taken as zero. The potential energy outside the particle, which determines the height of the well's wall, was set to $V_{ligands} = \left[E_{LH}(ligands) - E_{bg(ZnSe)} \right]/2$, where $E_{LH}(ligands)$ is the energy difference between the LUMO and HOMO energies of the ligand. For oleylamine, $E_{LH}(ligands) = 4.430 \, eV$.[8]

In this calculations, Coulomb, Exchange, and Correlation interactions were neglected as they were not easily obtained for elongated systems, and may further shift the exciton's energy. We took both the bulk band gap energy for ZnSe and ZnS and the effective masses from references[9-13], and are summarized in Table S2. The hole states correspond to the heavy hole, which dominates the valence band-edge states in this system.

Comparison between the electronic structure of hetero-ZnSe-ZnS/ZnS nanorod couples and homo- ZnSe was obtained for systems of similar ZnSe dimensions. All geometric parameters were

ZnSe rod couples dimensions

Short edge diameter 3 nm
Long edge length 77 nm
Long edge diameter 2 nm
Gap size 1 nm
Short edge length 5 nm
Total length 83 nm

ZnSe-ZnS (ZB)/ZnS (W) core/shell rod couples dimensions

ZnS (ZB) Diameter 5.6 nm
ZnSe and ZnS (W) length 74.4 nm
ZnSe diameter 2 nm
Gap size 1 nm
ZnS (W) diameter 5.6 nm
ZnS (ZB) length 12.2 nm
Total length 85.6 nm
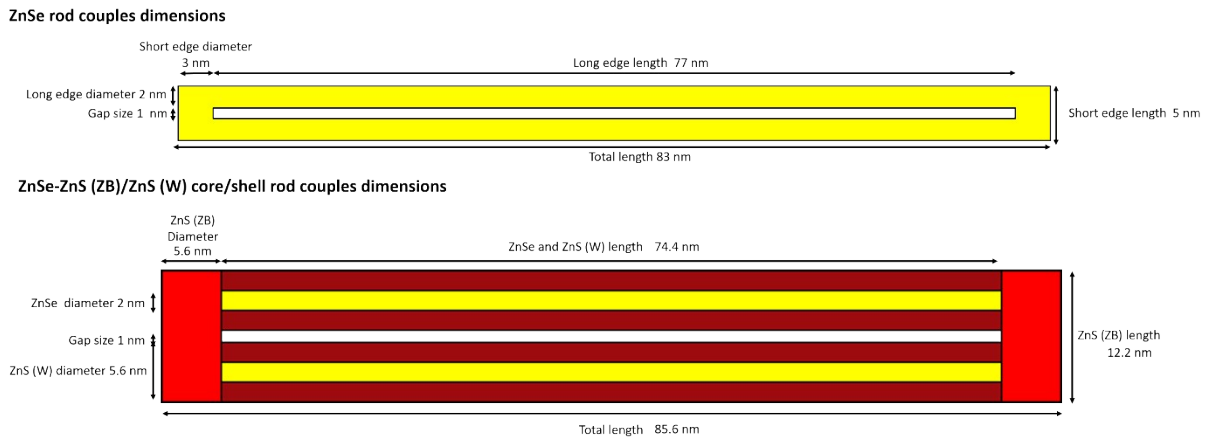
Scheme S1: Dimensions of the different systems used for calculating the electronic structures

set according to the dimensions extracted from TEM images and are shown in Scheme S1. The particles were embedded in an environment of organic material, with wave functions set to zero at

the boundaries. The environment dimensions were increased until the difference in eigenvalues was lower than 10^{-4} eV, omitting boundary artifacts on the solution. The energies and the contour of the wave functions cross section along the zx plane were shown in Figure 4 in the main article.

As discussed in the main article, in ZnSe nanorod couples, the wavefunctions of the lowest electron/hole states reside in the corners and hence occupy the short vertics, while in the hetero- ZnS-ZnSe nanorod couples they reside in the long vertices. In the hetero- ZnS-ZnSe system, in the first 6 states, the hole and electron occupies only ZnSe rod states. Interestingly, despite lying at the edge of the conduction-band ofset of ZnSe and ZnS (ZB), the electron also occupies ZnSe rod states, and this is because the first allowed state of the ZnS in the short edges has a much higher energy becuase of the confinement. However, the electron wavefunction panatrates the ZnS (W) shell quite significantly. Within the first 6 states, in the ZnSe there are several transitions that are well-defined because of the short/long edges states. In contrary, in the hetero- ZnS-ZnSe system, the states are almost degenerate because they are "rod" states. This difference can not be distinguished for the ensemble at room temperature but might be visible for single particles.

It should be noted that the model described above produces only a first approximation for the accurate energy values. In order to provide a more detailed picture of the electronic structure, including hole state mixing, electronic fine structure, and dipole moment induced effects, a more complex modeling is required, which is beyond the scope of the calculation described above.

Table S2. Bulk band gap energy and effective masses for ZnSe and ZnS

	ZnSe	ZnS (ZB)	ZnS (W)	Environment
m_e^*	$0.21\,m_e$	$0.22\,m_e$	$0.22\,m_e$	$1\,m_e$
m_{hh}^*	$0.67\,m_e$	$1.76\,m_e$	$1.4\,m_e$	$1\,m_e$
E_{bg}	2.82 eV	3.78 eV	3.91 eV	4.430 eV
V_e	0	0.51	0.56	0.7965 eV
V_h	0	0.45	0.53	0.7965 eV
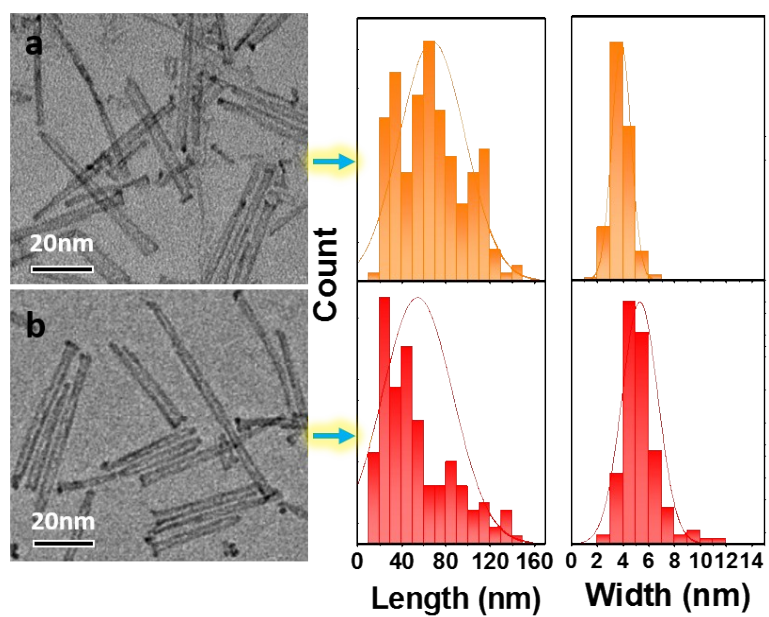
Figure S11. Sizing histograms of a) the original ZnSe nanorod couples before (top panel) (length 65.55 ± 25.40 nm × width 6.36 ± 1.54 nm) and b) after CdS shell growth (bottom panel) (length 51.90 ± 19.30 nm ×width 7.55 ± 1.42 nm).
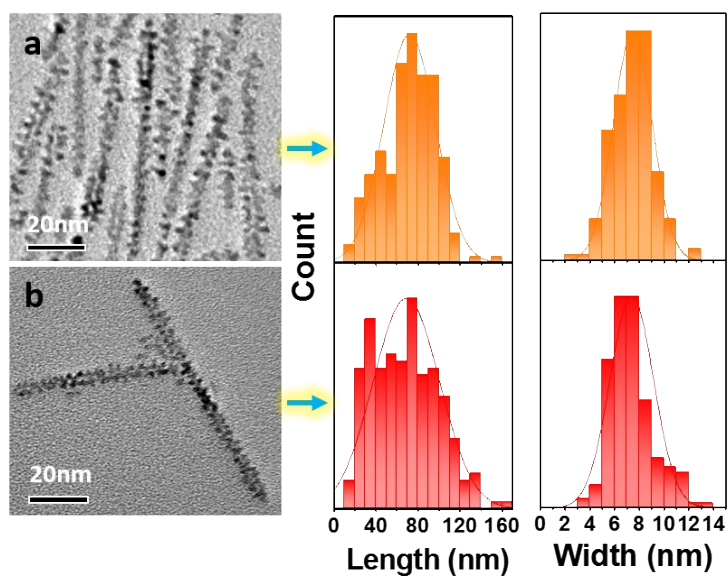
Figure S12. Sizing histograms of a) the original branched hetero- ZnS-ZnSe/ZnS nanorod couples before (top panel) (length 88.58 ± 26.93 nm ×width 7.47 ± 1.55 nm) and b) after CdS shell growth (bottom panel) (length 83.51 ± 28.50 nm ×width 7.51 ± 2.71 nm).
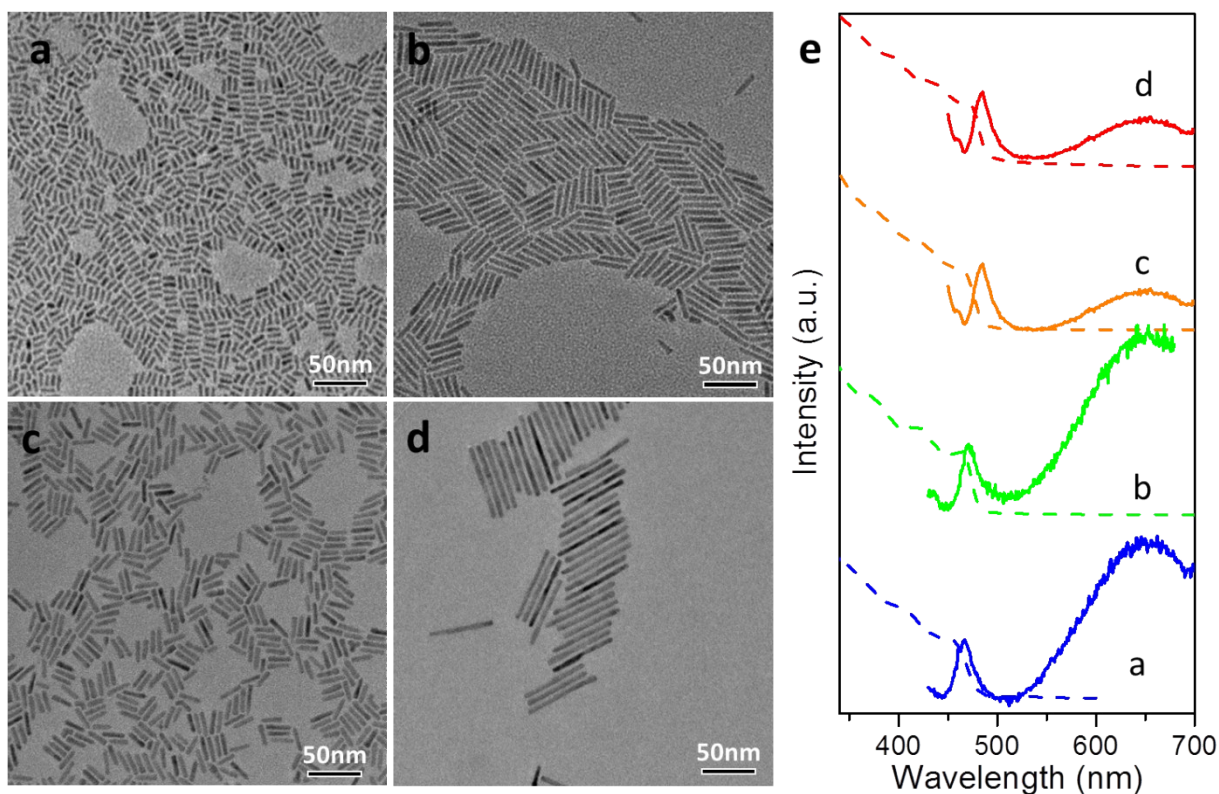
Figure S13. TEM images of CdS nanorods synthesized in TOP/TOPO using hexylphosphonic acid as the surfactant. (a-d) TEM images of CdS nanorods. (a) 3.8 nm (width) × 11 nm (length). (b) 4.5 nm (width) × 32 nm (length). (c) 5.5 nm (width) × 23 nm (length). (d) 4.7 nm (width) × 72 nm (length). (e) Absorption (dashed line) and luminescence (solid line) of CdS nanorods.

To further elucidate the origin of the blue emission of hetero- ZnS-ZnSe/ZnS/CdS core/shell/shell nanorods couples, a control experiment for the synthesis of CdS nanorods was conducted using similar synthetic conditions as those for the CdS shell growth on the ZnSe nanoparticle. All obtained CdS nanorods show a very weak band edge emission in the range of 460 nm to 476 nm and a broad band trap state emission at longer wavelengths with the luminescence quantum efficiency less than 0.1%.
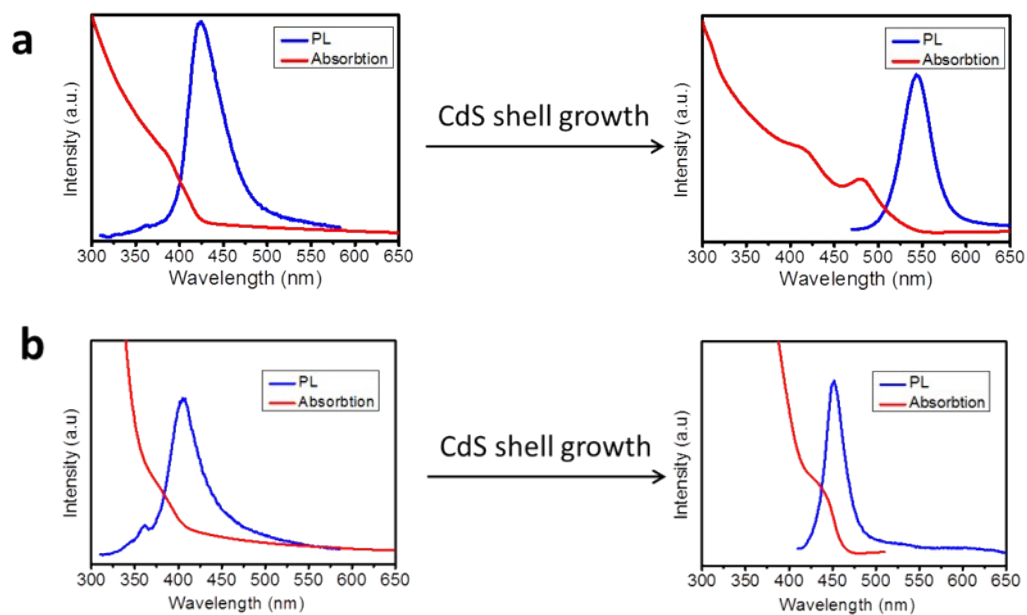
Figure S14. Comparison of absorption and luminescnece spectra of nanorod couples before and after CdS shell growth. (a) Homo- ZnSe/CdS core/shell nanorod couples. (b) Hetero- ZnS-ZnSe/ZnCdS core/shell/shell nanorod couples.
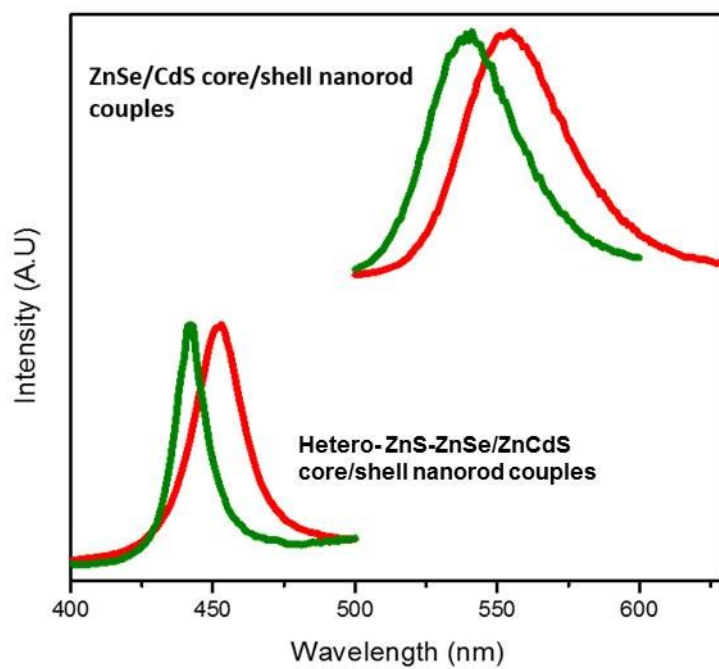
Figure S15. PL spectra of nanorods couples with the CdS shell at room temperature (red curves) and 77K (green curves).
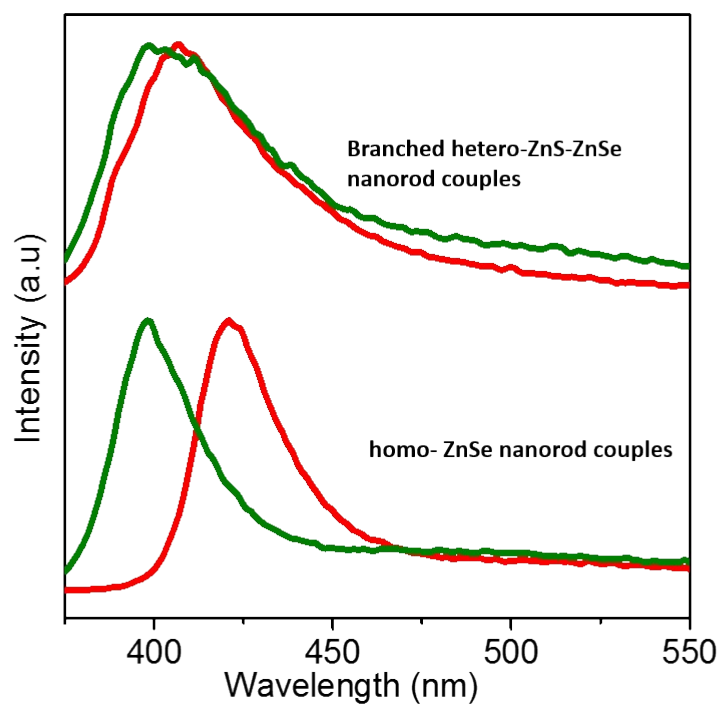
Fig S16. PL spectra of nanorods couples after surface ligand exchange with TOP at room temperature (red curves) and 77K (green curves).
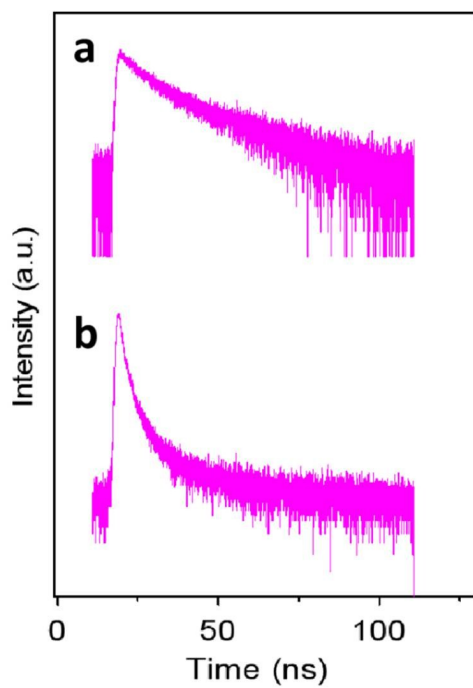
Figure S17. Comparison of 77 K fluorescence lifetime decay curves of hetero-ZnS-ZnSe/ZnCdS and homo- ZnSe/CdS core/shell nanorod couples.

Table S3 Comparison of optical properties of core/shell nanorod couples.

With CdS Shell	Emission (nm)	τ_1 (ns)	τ_2 (ns)	τ_1 percentage	Quantum Yields (%)
Hetero- nanorod couples (RT)	453	6.0	45.3	8%	2.3
Hetero- nanorod couples (77K)	442	2.5	12.1	46%	-
Homo- nanorod couples (RT)	554	10.3	50.5	20%	15.4
Homo- nanorod couples (77K)	540	7.3	32.4	18%	-
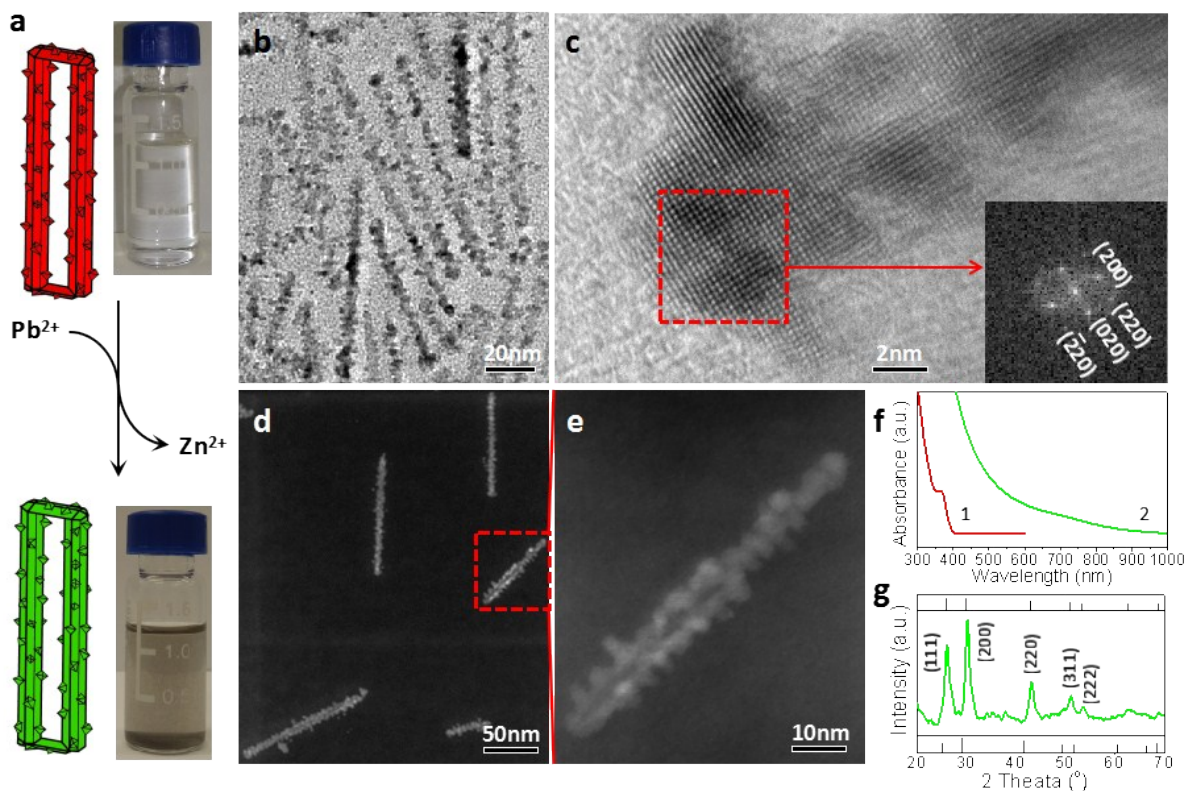
Figure S18. Branched hetero- PbS-PbSe/PbS nanorod couples obtained by a cation exchange reaction. (a) Schematic illustration of branched hetero- PbS-PbSe nanorod couples generated through Zn^{2+} replacement by Pb^{2+}. Band gap tuning is visualized by the color change of nanoparticle solutions before and after the cation exchange. (b) TEM image (c) HRTEM image. Inset in (c) shows the FFT of a selected area labelled by a red rectangle. (d,e) HAADF-STEM images of branched hetero- PbS-PbSe nanorod couples. (f) Comparison of optical absorption spectra of the branched hetero- PbS-PbSe nanorod couples before and after the cation exchange. (g) XRD patterns of branched hetero- PbS-PbSe nanorod couples. The standard XRD patterns for PbSe (bottom) and PbS (top) are given for reference.
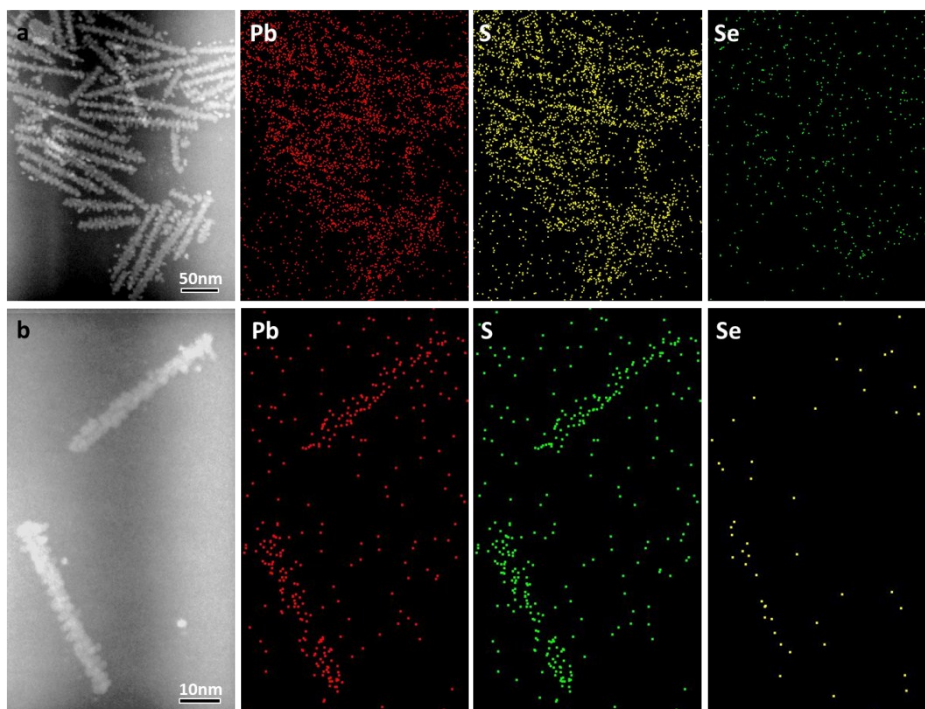
Figure S19. HAADF-STEM images and element maps of branched hetero- PbS-PbSe/PbS core/shell nanorod couples obtained after the cation exchange reaction. (a) Hetero- PbS-PbSe/PbS core/shell nanorod couples with a large population. (b) Two individual hetero- PbS-PbSe/PbS core/shell nanorod couples.

References

1 L. Carbone, C. Nobile, M. De Giorgi, F. Della Sala, G. Morello, P. Pompa, M. Hytch, E. Snoeck, A. Fiore, I. R. Franchini, M. Nadasan, A. F. Silvestre, L. Chiodo, S. Kudera, R. Cingolani, R. Krahne and L. Manna, *Nano Lett.*, 2007, **7**, 2942-2950.

2 G. Jia, A. Sitt, G. B. Hitin, I. Hadar, Y. Bekenstein, Y. Amit, I. Popov and U. Banin, *Nat. Mater.*, 2014, **13**, 301-307.

3 A. M. Smith, A. M. Mohs and S. Nie, *Nat. Nanotechnol.*, 2009, **4**, 56-63.

4 H. Zhong, T. Mirkovic and G. D. Scholes, Comprehensive Nanoscience and Technology Vol. 5: Nanocrystal Synthesis, (Eds: D. Andrews, G. Scholes, G. Wiederrecht), Elsevier 2010, 153-201.

5 C.-M. Ning, L. Dou and P. Yang, *Nat. Rev. Mater.*, 2017, **2**, 17070.

6 C. Tan, J. Chen, X.J. Wu and H. Zhang, *Nat. Rev. Mater.*, 2018, **3**, 17089.

7 G. Pellegrini, G. Mattei, P. and Mazzoldi, *J. Appl. Phys.*, 2005, **97**, 073706.

8 T. Omata, K. Nose and S. Otsuka-Yao-Matsuo, *J. Appl. Phys.*, 2009, **105**, 073106.

9 a) H. Landolt, R. Börnste and Landolt-Börnstein: Numerical Data and Functional Relationships in Science and Technology, O. Madelung, U. Rössler, M. Schulz, Ed. group III, vol. 41B (Springer, Berlin, 1982); b) Landolt-Börnstein: Numerical Data and Functional Relationships in Science and Technology, New Series (Ed: K. H. Hellwege), Springer, Berlin 1983.

10 M. Cardona, *J. Phys. Chem. Solid.*, 1963, **24**, 1543-1555.

11 S.H. Wei and A. Zunger, *Appl. Phys. Lett.*, 1998, **72**, 2011-2013.

12 H. E. Ruda, *J. Appl. Phys.*, 1986, **59**, 3516-3526.

13 Murayama, M. and Nakayama, T. *Phys. Rev. B* 1994, **49**, 4710-4724.